Study of the self-degradation performance of a passive direct methanol fuel cell with Fe-N-C catalyst

Chenjun Hou[a], Weijian Yuan[a,*], Shilong Gao[b], Yujun Zhang[a], Yufeng Zhang[a], and Xuelin Zhang [a,*]

a School of Astronautics, Harbin Institute of Technology, Harbin, China

b State Key Laboratory of Organic-Inorganic Composites, Beijing Advanced Innovation Center for Soft Matter Science and Engineering, Beijing University of Chemical Technology, Beijing, 100029, People's Republic of China

E-mail: ywj@hit.edu.cn (Weijian Yuan); zhangxuelin@hit.edu.cn (Xuelin Zhang)

Supporting Information

1. Experiment

1.1 Chemicals

Aniline (99.0% purity) and monocyanamide (49.0% purity) were purchased from Aladdin. hydrochloric acid (HCl, 37%) was purchased from Kermel, and carbon black BP2000 was donated by Cabot Corp. Ferric chloride ($FeCl_3$, 98% purity) and ammonium persulfate ($(NH_4)_2S_2O_8$, 98% purity) were purchased from Alfa Aesar.

1.2 Synthesis of Fe-N-C catalysts

2 ml aniline and 3 ml monocyanamide were dissolved in 80 ml 1.5 M HCl, and 0.4 g carbon black with 3 g $FeCl_3$ were dispersed in 80 ml 1.5 M HCl. The above two solutions were mixed, and then 5 g $(NH_4)_2S_2O_8$ dissolved in 80 ml 1.5 M HCl was added. After polymerization, a heat treatment in 900 °C under N_2 for 1 h was conducted, and the product was pre-leached in 2 M H_2SO_4 at 90 °C for 5 h. The pre-leached powder then underwent a second heat treatment under N_2 for 2.5 h and under NH_3 for 0.5 h in 900 °C.

1.3 Characterizations

Scanning electron microscope (SEM) was conducted to observe the morphology of prepared catalysts, and X-ray diffraction (XRD) and Raman spectroscopy were performed to analyze the physical structures and disordered degree of catalysts separately. N_2 adsorption/desorption test was applied to character the porous structures of catalysts, and X-ray photoelectron spectroscopy (XPS) measurement was utilized to research the chemical components of catalysts.

1.4 Electrochemical measurements

The system of electrochemical measurement was composed of a glassy carbon working electrode, a platinum foil counter electrode and an Hg/Hg_2SO_4 reference electrode. The working electrodes were prepared by coating the catalyst ink onto the surface of glassy carbon electrode. Particularly, 15 mg Fe-N-C catalyst, 525 μL ethanol and 145 μL Nafion solution (5%) were mixed and stirred for 30 minutes, and then, 7 μL catalyst ink was applied onto the working electrode, making the loading of Fe-N-C catalyst 800 μg cm^{-2}. As a comparison, 5 mg 40% Pt/C catalyst, 1.21 mL isopropanol and 40 μL Nafion were well mixed, and 5 μL of catalyst ink was coated on the working electrode, making the loading of Pt 80 μg cm^{-2}.

Electron transfer numbers can be calculated according to the Koutecky-Levich (K-L) equation, which can be expressed as:

$$1/j=1/j_k + 1/j_d = 1/j_k + 1/(0.62nFD^{2/3}v^{-1/6}C\omega^{1/2}) \quad (1)$$

where j is the total current density, j_k is the kinetic current density and j_d is the diffusion limiting current density. K-L equation relates the liming current density measured in RDE tests and the number of electron transfer (n), the rotation speed (ω) and other parameters including F, the Faraday constant (96485 C mol^{-1}); D, the diffusion coefficient of oxygen ($1.93*10^{-5}$ cm^2 s^{-1}); v, the electrolyte kinematic viscosity ($1*10^{-2}$ cm^2 s^{-1}); and C, the bulk oxygen concentration ($1.26*10^{-3}$ mol dm^{-3}). For rotating ring disk electrode (RRDE) test, the ring potential was kept as 1.2 V vs RHE, and the H2O2 yield was calculated according to the Equation (2):

$$\%H_2O_2 = 100 \cdot \frac{\frac{2I_r}{N}}{I_d + \frac{I_r}{N}} \quad (2)$$

where: I_d, I_r and N represent the disk current, the ring current and the ring collection efficiency (0.37). RRDE tests were performed under 1600 rpm at 10 mV s^{-1}.

2. Figures

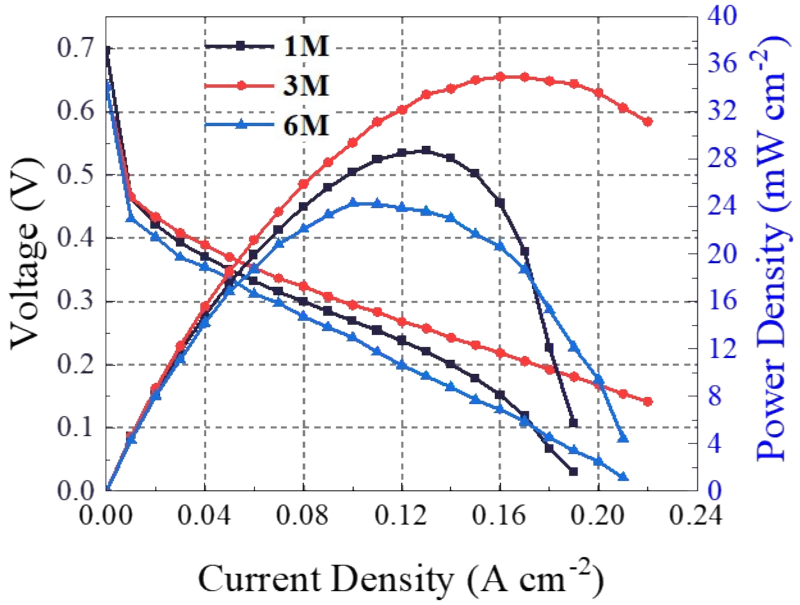

Fig. S1 Polarization curves of Pt/C based DMFC at 60 °C.

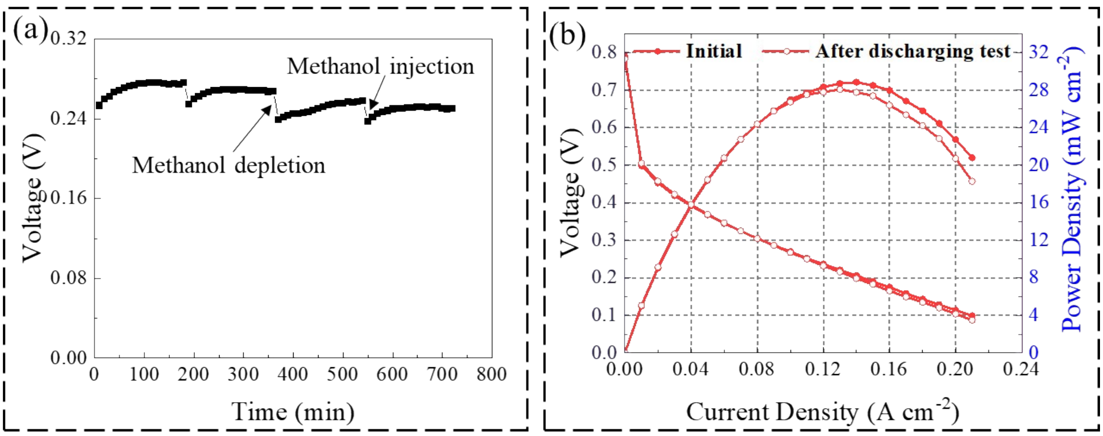

Fig. S2 Discharging curve of a DMFC with a constant current density of 100 mA cm^{-2} within 12 hours (a); Polarization curves of a DMFC before and after the stability test (b). The working temperature is 60 °C and the methanol concentration is 3 M.

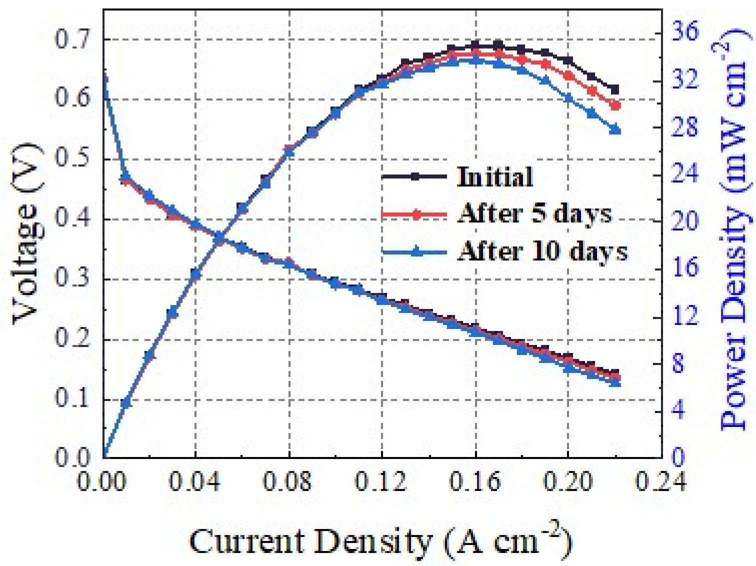

Fig. S3 Polarization curves of Pt/C based DMFC after stationary over several days.

The concentration of supplied methanol is 3 M and the temperature is 60 °C.

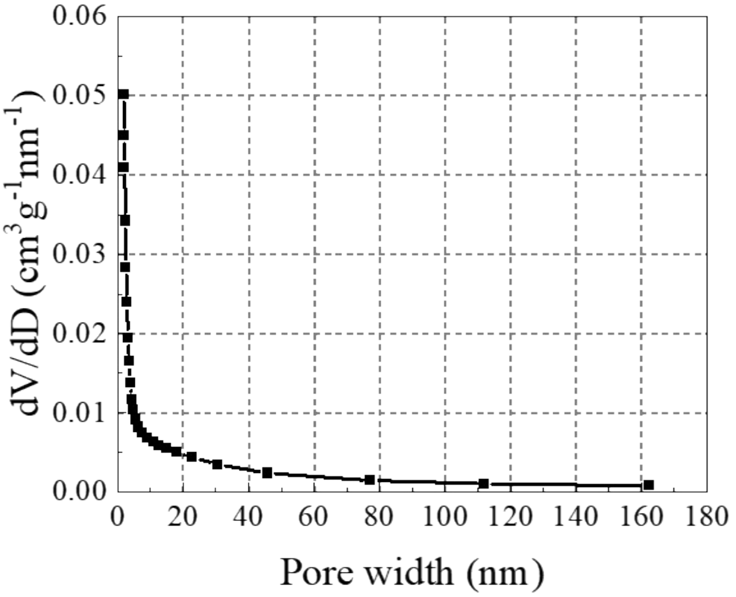

Fig. S4 Pore size contribution curve of prepared Fe-N-C catalyst

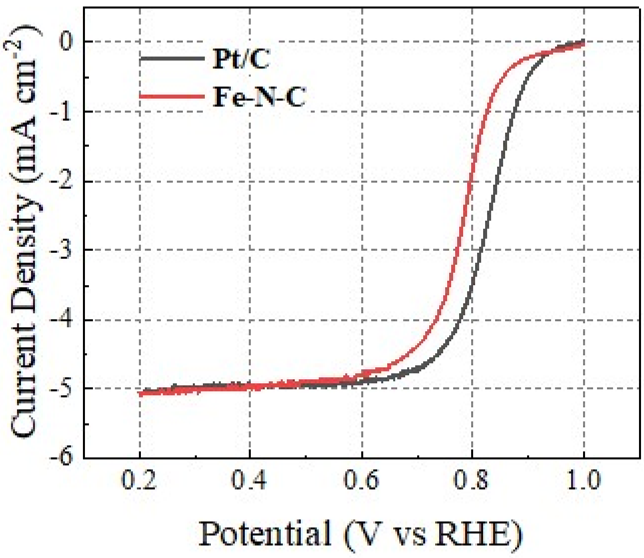

Fig. S5 LSV curves of catalysts tested in O_2-satuarated 0.1M $HClO_4$.

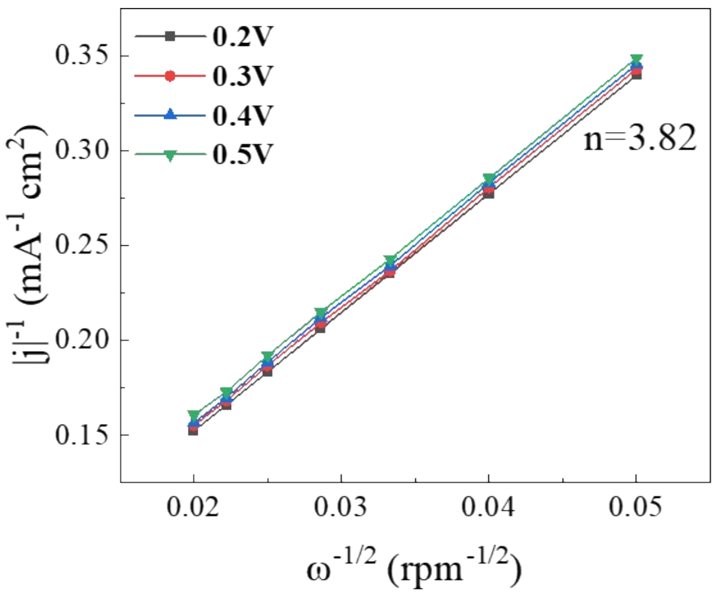

Fig. S6 Koutecky-Levich plots of Fe-N-C tested in O_2-satuarated 0.1 M $HClO_4$

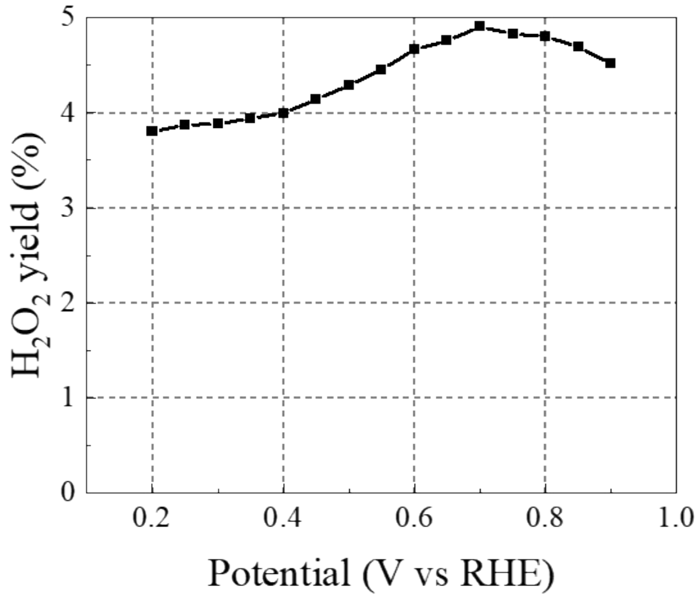

Fig. S7 H_2O_2 yield of the prepared Fe-N-C catalyst in O_2-satuarated 0.1 M $HClO_4$

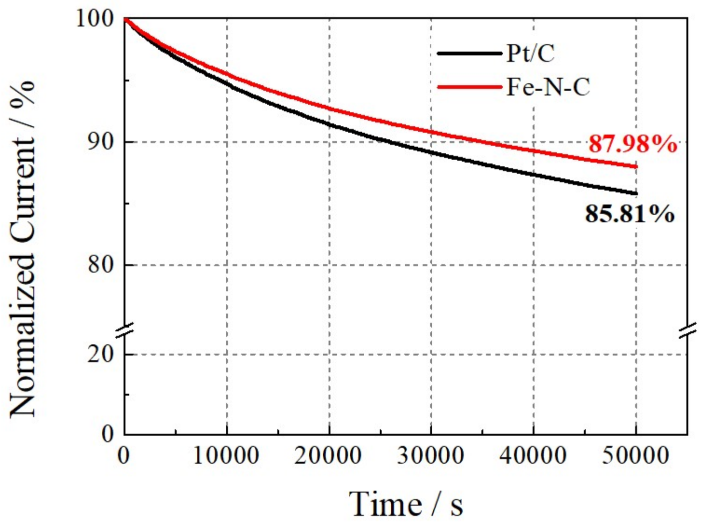

Fig. S8 I-t curves of Pt/C catalyst and Fe-N-C catalyst tested in O_2-satuarated 0.1 M $HClO_4$ at 0.5 V vs RHE.

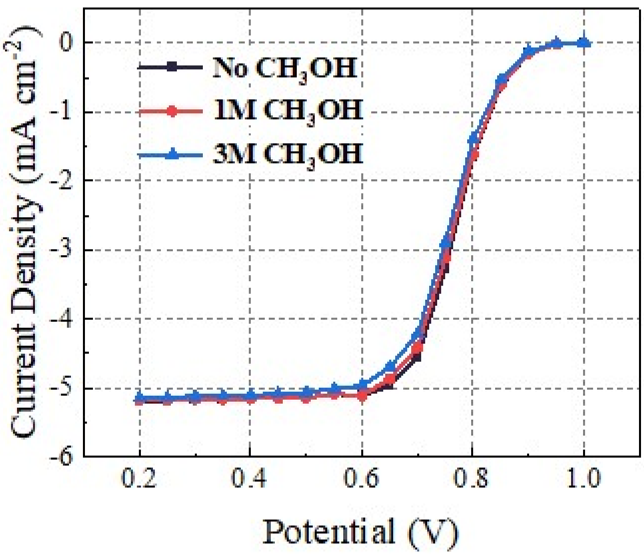

Fig. S9 SCV curves of Fe-N-C based electrode tested in O_2-satuarated 0.1M $HClO_4$ with the addition of methanol.

Table S1 Summary of the component and performance of PEM-based DMFC with Fe-N-C based cathode catalyst

Cathode	Anode	Reactant	Performance	Ref.
5.0 mg/cm^2 50% Nafion	4.0mg/cm^2 PtRu/C	3M CH_3OH 1mL/min O_2,100 mL/min	80℃ 130 mW/cm^2	1
2.5mg/cm^2 50% Nafion	1.0 mg/cm^2 Pt/C	2M CH_3OH 1mL/min O_2,200 mL/min	90℃ 20 mW/cm^2	2
4.5 mg/cm^2 45%Nafion	1.0 mg/cm^2 PtRu/C	10M CH_3OH2mL/min O_2,100 mL/min	90℃ 48 mW/cm^2	3
2.5 mg/cm^2 45%Nafion	2.5 mg/cm^2 PtRu/C	5M CH_3OH 2mL/min O_2,100 mL/min	110℃ 11.2 mW/cm^2	4
4.0 mg/cm^2 45%Nafion	1.0 mg/cm^2 PtRu/C	2M CH_3OH 2mL/min O_2,100 mL/min	90℃ 10.5 mW/cm^2	5
3.0 mg/cm^2 45%Nafion	1.0 mg/cm^2 PtRu/C	10M CH_3OH 2mL/min O_2,100 mL/min	90℃ 22 mW/cm^2	6
7.4 mg/cm^2 45%Nafion	1.0 mg/cm^2 PtRu/C	10M CH_3OH 2mL/min O_2,100 mL/min	90℃ 30 mW/cm^2	7
5.0 mg/cm^2 66.7%Nafion	2.0 mg/cm^2 PtRu/C	1M CH_3OH 2mL/min O_2,400 mL/min	80℃ 32 mW/cm^2	8
4.0mg/cm^2 25%Nafion	1.5 mg/cm^2 PtRu/C	2M CH_3OH 20mL/min O_2,500 mL/min	50℃ 20.9 mW/cm^2	9
4.0 mg/cm^2 45%Nafion	4.0 mg/cm^2 PtRu/C	10M CH_3OH 2mL/min O_2,100 mL/min	90℃ 60 mW/cm^2	10
5.0 mg/cm^2 50%Nafion	2.0 mg/cm^2 PtRu/C	5M CH_3OH 10mL/min O_2,25 mL/min	20℃ 6 mW/cm^2	11
4.0 mg/cm^2 45%Nafion	2.7 mg/cm^2 PtRu/C	0.5M CH_3OH 1.8mL/min Air,500 mL/min	75℃ 58 mW/cm^2	12
5.0 mg/cm^2 50%Nafion	2.0 mg/cm^2 PtRu/C	1M CH_3OH 2.5mL/min Air,100 mL/min	70℃ 14.9 mW/cm^2	13
4.0 mg/cm^2 45%Nafion	4.0 mg/cm^2 PtRu/C	2M CH_3OH Air-breathing	60℃ 19.48 mW/cm^2	14
5.0 mg/cm^2 50%Nafion	4.0 mg/cm^2 PtRu/C	1M CH_3OH Air-breathing	30℃ 11.72 mW/cm^2	15
8.0 mg/cm^2 **45%Nafion**	**4.0 mg/cm^2** **PtRu/C**	**3M CH_3OH** **Air-breathing**	**60℃** **28.85 mW/cm^2**	**This Work**

Table S2 Summary of the performance of the PEM-based DMFC with Fe-N-C and Pt/C cathode catalysts

P_{max}@Fe-N-C	P_{max}@Pt/C	Tem.	P_{max}@Fe-N-C/ P_{max}@Pt/C	Ref.
6.5 mW/cm^2	11.1 mW/cm^2	30°C	58.6%	[7]
22.6 mW/cm^2	30.9mW/cm^2	90°C	73.1%	[16]
19.6 mW/cm^2	30.9mW/cm^2	90°C	63.4%	[2]
38.47 mW/cm^2	60 mW/cm^2	70°C	64.1%	[17]
71 mW/cm^2	115 mW/cm^2	80°C	61.7%	[18]
19.48 mW/cm^2	33.95mW/cm^2	60°C	57.4%	[14]
58 mW/cm^2	120 mW/cm^2	60°C	48.3%	[12]
21.5 mW/cm^2	115 mW/cm^2	70°C	18.7%	[19]
28.85 mW/cm^2	**34.94 mW/cm^2**	**60°C**	**82.6%**	**This Work**

Reference:

1. Y.-C. Wang, L. Huang, P. Zhang, Y.-T. Qiu, T. Sheng, Z.-Y. Zhou, G. Wang, J.-G. Liu, M. Rauf, Z.-Q. Gu, W.-T. Wu and S.-G. Sun, *ACS Energy Letters*, 2017, **2**, 645-650.
2. L. Osmieri, R. Escudero-Cid, A. H. A. Monteverde Videla, P. Ocón and S. Specchia, *Applied Catalysis B: Environmental*, 2017, **201**, 253-265.
3. D. Sebastián, A. Serov, K. Artyushkova, J. Gordon, P. Atanassov, A. S. Aricò and V. Baglio, *ChemSusChem*, 2016, **9**, 1986-1995.
4. A. H. A. Monteverde Videla, D. Sebastián, N. S. Vasile, L. Osmieri, A. S. Aricò, V. Baglio and S. Specchia, *Int. J. Hydrogen Energy*, 2016, **41**, 22605-22618.
5. C. Lo Vecchio, A. Aricò and V. Baglio, *Materials*, 2018, **11**.
6. D. Sebastián, A. Serov, K. Artyushkova, P. Atanassov, A. S. Aricò and V. Baglio, *J. Power Sources*, 2016, **319**, 235-246.
7. D. Sebastián, V. Baglio, A. S. Aricò, A. Serov and P. Atanassov, *Applied Catalysis B: Environmental*, 2016, **182**, 297-305.
8. J. C. Park and C. H. Choi, *J. Power Sources*, 2017, **358**, 76-84.
9. Y. Hu, J. Zhu, Q. Lv, C. Liu, Q. Li and W. Xing, *Electrochim. Acta*, 2015, **155**, 335-340.
10. D. Sebastián, A. Serov, I. Matanovic, K. Artyushkova, P. Atanassov, A. S. Aricò and V. Baglio, *Nano Energy*, 2017, **34**, 195-204.
11. S. Baranton, C. Coutanceau, J. M. Léger, C. Roux and P. Capron, *Electrochim. Acta*, 2005, **51**, 517-525.

12. Q. Li, T. Wang, D. Havas, H. Zhang, P. Xu, J. Han, J. Cho and G. Wu, *Advanced Science*, 2016, **3**.

13. R. Mei, J. Xi, L. Ma, L. An, F. Wang, H. Sun, Z. Luo and Q. Wu, *J. Electrochem. Soc.*, 2017, **164**, F1556-F1565.

14. X. Zhang, C. Hou, W. Yuan, C. Deng, F. Ji, L. Tian, G. Lin, H. Deng and Y. Zhang, *Fuel Cells*, 2022, **23**, 42-50.

15. J. Xi, F. Wang, R. Mei, Z. Gong, X. Fan, H. Yang, L. An, Q. Wu and Z. Luo, *RSC Advances*, 2016, **6**, 90797-90805.

16. L. Osmieri, R. Escudero-Cid, M. Armandi, A. H. A. Monteverde Videla, J. L. García Fierro, P. Ocón and S. Specchia, *Applied Catalysis B: Environmental*, 2017, **205**, 637-653.

17. L. Cao, W. Yang, H. Zou, S. Chen and Z. Liu, *J. Inorg. Organomet. Polym. Mater.*, 2019, **29**, 1886-1894.

18. X. Xu, X. Zhang, Z. Xia, R. Sun, J. Wang, Q. Jiang, S. Yu, S. Wang and G. Sun, *ACS Appl. Mater. Interfaces*, 2021, **13**, 16279-16288.

19. E. Giordano, E. Berretti, L. Capozzoli, A. Lavacchi, M. Muhyuddin, C. Santoro, I. Gatto, A. Zaffora and M. Santamaria, *J. Power Sources*, 2023, **563**.